

Motion of spin polariton bullets in semiconductor microcavities

C. Adrados,¹ T. C. H. Liew,² A. Amo,^{1,3} M. D. Martín,⁴ D. Sanvitto,^{4,5}
C. Antón,⁴ E. Giacobino,¹ A. Kavokin,^{6,7} A. Bramati,¹ and L. Viña⁴

¹Laboratoire Kastler Brossel, Université Pierre et Marie Curie, École Normale Supérieure et CNRS,
UPMC Case 74, 4 place Jussieu, 75252 Paris Cedex 05, France

²Institute of Theoretical Physics, Ecole Polytechnique Fédérale de Lausanne, CH-1015, Lausanne, Switzerland

³CNRS-Laboratoire de Photonique et Nanostructures, Route de Nozay, 91460 Marcoussis, France

⁴Departamento de Física Materiales and Instituto de Ciencias de Materiales 'Nicolás Cabrera',
Universidad Autónoma de Madrid, Cantoblanco, E-28049 Madrid, Spain

⁵NNL, Istituto Nanoscienze - CNR, Via Arnesano, 73100 Lecce, Italy

⁶Laboratoire Charles Coulomb UMR 5221 CNRS-UM2 F-34095 Montpellier Cedex 5, France

⁷Physics and Astronomy School, University of Southampton, Highfield, Southampton, SO171BJ, UK

(Dated: July 2, 2021)

The dynamics of optical switching in semiconductor microcavities in the strong coupling regime is studied using time- and spatially-resolved spectroscopy. The switching is triggered by polarised short pulses which create spin bullets of high polariton density. The spin packets travel with speeds of the order of 10^6 m/s due to the ballistic propagation and drift of exciton-polaritons from high to low density areas. The speed is controlled by the angle of incidence of the excitation beams, which changes the polariton group velocity.

PACS numbers: 71.36.+c, 71.35.Gg, 78.67.De

Introduction.— Compact, solid-state, semiconductor systems are amongst the most promising candidates for the construction of optical signal processing devices (see [1] and references therein). Often it is desirable to hybridize the abilities of electronic excitations with those of light, for example in semiconductor microcavities, where exciton-polaritons arise from strong coupling between cavity photons and quantum well excitons [2]. The strong polariton-polariton interactions yield rich nonlinearities capable of creating individual optical switches [1, 3–5] and memory elements [6, 7] with low threshold power. Their short lifetime underlies a high speed ps dynamics, capable of ultra-fast switching [8–10].

Unfortunately, a problem arises when one considers how to link multiple polariton-based switches into an optical circuit. Many theoretical proposals rely on using ballistically propagating polaritons to carry information [11–13]. Here the short polariton lifetime seems to become a drawback since it introduces a signal loss mechanism, implying that some kind of signal amplification is necessary. An alternative to ballistic propagation is the use of 'polariton neurons' in a microcavity excited in the bistable regime [14], where signals are carried by the propagation of a domain wall separating regions in which the system is locally in the low or high density stable states. The propagation is expected to be confined along channels and the signal propagation distance limited by the size of a background optical pump, oriented at normal incidence, rather than the polariton lifetime.

Another important feature of polaritons is their spin degree of freedom, which allows their application in spinoptronic devices; polaritons exhibit one of two spin states ($\sigma^{+/-}$) that couple to external circularly polarized light and can be used to encode information instead of

relying on intensity. Furthermore, the Coulomb interaction between polaritons depends on their spin state. It is usually assumed that the interaction constant between polaritons with parallel spins is larger than the interaction constant between polaritons with antiparallel spins [15–18]. This allows spin dependent switching to occur [1, 3–5, 7].

In this work we merge the concepts of ballistic signal propagation and polariton neurons, in the route towards the realization of the recently proposed spin-optronic devices [11–13]. Excitation with a continuous wave (*cw*) optical pump at an angle supports the triggering of a propagating bullet, which travels across the pump spot for distances much longer than allowed by the polariton lifetime, thus overtaking a drawback for the implementation of realistic devices. The bullet corresponds to a temporary switch from the low intensity (*off*) state to the high intensity (*on*) state in a highly non-linear regime. The signal propagation speed is approximately given by the polariton group velocity, which is controlled by variation of the optical excitation angle. Our temporally and spatially resolved measurements are fully supported by a theoretical model based on the Gross-Pitaevskii (GP) equation [14, 20].

Experiment.— Our experiment consists in switching a polariton fluid, quasi-resonantly created in a GaAs microcavity (with Rabi-splitting 5.1 meV) with a *cw* Ti:Sa laser pump, from the *off* to the *on* state by the application of a weak triggering probe pulse (2 ps-long pulses every 12 ns). The pump (FWHM 100 μm) and probe (FWHM 20 μm) beams impinge on the microcavity, at a point where the cavity-exciton detuning is approximately zero, with the same angle, the latter positioned in such a way that the propagating polaritons are able to cross

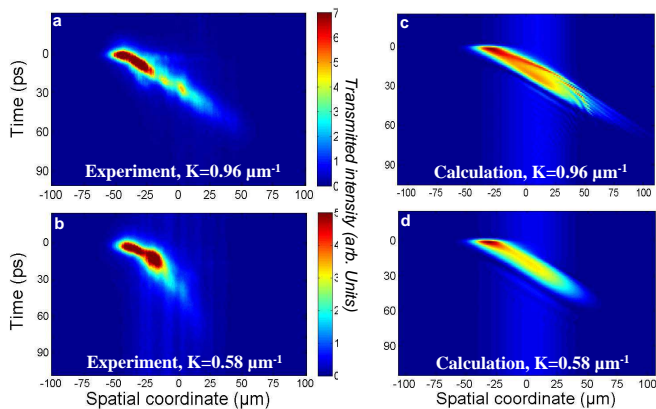


FIG. 1: Streak camera (5 ps - time resolution) images of the near-field polariton intensity in space and time for excitation wavevectors $0.96 \mu\text{m}^{-1}$ (a) and $0.58 \mu\text{m}^{-1}$ (b). Corresponding theoretical images from the Gross-Pitaevskii equations are shown in (c) and (d).

the pump beam area from one side to the other [1].

The *cw* pump has a Gaussian profile in space and is blue detuned by 0.5 nm from the lower polariton branch resonance, which is at 837 nm at the chosen point of the sample. The central wavelength of the pulsed probe (duration of 2 ps, spectral width of 1.2 nm) matches the wavelength of the pump. We will start by considering a circularly polarized pump and a co-circularly polarized probe. In this case the system effectively simplifies to a scalar system. As the pump power is increased, a nonlinear threshold can be seen in the transmitted intensity [1, 19]. Above threshold the whole transmitted beam has a top-hat-like profile and is no longer Gaussian. Under these conditions bright polariton bullets cannot be excited, so we instead choose the pump power to be below the nonlinear threshold.

As shown in Ref. [1], a small *cw* probe of enough power, inside the large pump would result in the switch to the *on* state of the whole pump spot. The region excited by the probe will be the first to switch to the *on* state. The ballistic propagation of the injected polaritons to the neighbouring region set by their propagation direction would then result in the switching *on* of the rest of the pump spot, in a relay mechanism. Thus, we expect the propagation to take place at the group velocity set by the in-plane wavevector of the pump. We can test the validity of this mechanism using a pulsed probe. The arrival of the probe will create a polariton bullet in the *on* state, which will propagate across the pump spot. In our experiments we follow the movement of these *on* polariton packets with a synchroscan streak camera, gaining access to the propagation speed.

Figures 1a and 1b display raw images from the streak camera directly showing the motion of the polariton bullet for two different in-plane wavevectors: $0.96 \mu\text{m}^{-1}$ and $0.58 \mu\text{m}^{-1}$ respectively. In the first case the bullet prop-

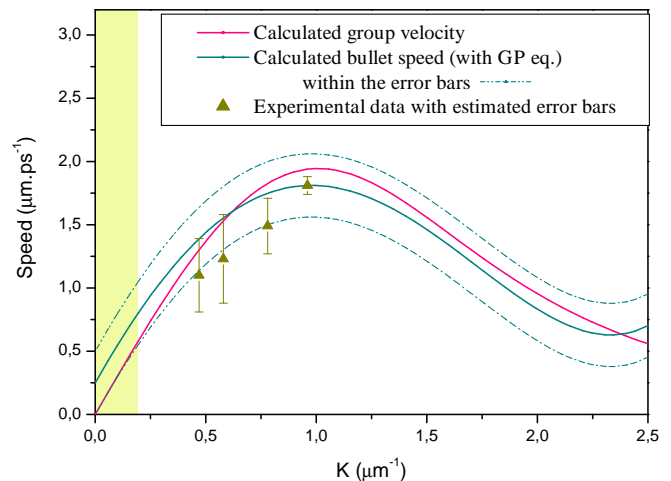


FIG. 2: Dependence of the signal propagation speed on the in-plane wavevector. Triangles show the experimentally measured points. The red curve shows the polariton group velocity, $v_g(k) = \frac{1}{\hbar} \frac{d}{dk} E_{\text{LPB}}(k)$. The solid blue curve shows the signal propagation speed estimated from the solution of the Gross-Pitaevskii equations. The dashed blue curves depict the confidence bands of the estimation. The yellow part indicates a wavevector slot where the error bars are too big for the behaviour of the signal speed to be analyzed properly.

agates across the entire *cw* pump spot and for a time much longer (the signal over noise ratio is bigger than 100 during 55 ps) than the polariton lifetime (~ 8 ps in our sample). These effects cannot be explained neglecting nonlinear interaction between the pump and probe and considering the propagation of the probe pulse only. For smaller in-plane wavevector, the bullet is more difficult to distinguish since it does not propagate such a large distance.

The slope of the emitted intensity shown in Fig. 1a and b can be used to estimate the signal propagation speed as $1.81 \pm 0.07 \mu\text{m.ps}^{-1}$ and $1.23 \pm 0.35 \mu\text{m.ps}^{-1}$, respectively. To first order, these values roughly match the expected polariton group velocity as shown in Fig. 2.

Considering the size and shape of the pump beam at high power with $K = 0.96 \mu\text{m}^{-1}$ and the measured speed of the polariton bullet, its lifetime matches the time to travel a $100 \mu\text{m}$ distance at $1.81 \mu\text{m.ps}^{-1}$. Note that the polariton lifetime and pulse duration do not have a significant effect on the bullet propagation speed. Nevertheless, they can play a role in the *on* to *off* switching process. Indeed a given region remains in the *on* state as long as the probe beam (directly or indirectly via relay-polaritons) feeds it. Hence, when the polaritons of this *on* region leave or decay via photon emission, the region falls back to the *off* state provided that the pulse of the probe beam is finished. Here we note that although the pump beam is blue-detuned with respect to the lower polariton resonance and one might expect to be in a bistable regime, due to the fact that polaritons are propagating,

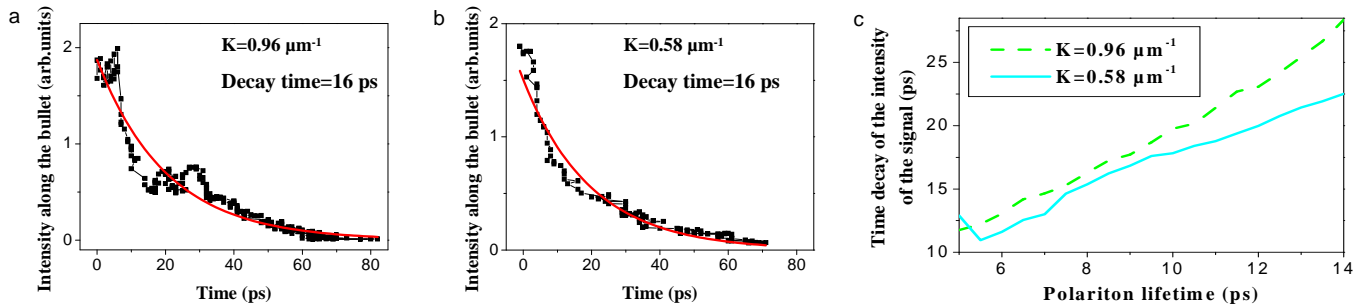


FIG. 3: a)/b) Time dependence of the intensity (integrated over $\sim 10^7$ single pulse realisations) of the polariton bullet observed experimentally for $K = 0.96 \mu\text{m}^{-1}/K = 0.58 \mu\text{m}^{-1}$. The solid red lines are exponential fits of the data. c) The dashed/solid lines represent the theoretical dependence of the polariton bullet decay time on the polariton lifetime for $K=0.96/0.58 \mu\text{m}^{-1}$.

there is no hysteresis. Essentially, the state of the system in a given region in space no longer depends on the history of that region, but rather on that of the neighboring regions from which polaritons arrive.

The lifetime of the bullet can be measured by tracking its intensity as it propagates. Figures 3a and 3b depict the intensity decays corresponding to Figs. 1a and b respectively. An exponential fit gives a decay time, τ , of about 16 ps, during which the bullets have traveled $\sim 30 \mu\text{m}/\sim 20 \mu\text{m}$ for $K = 0.96 \mu\text{m}^{-1}/K = 0.58 \mu\text{m}^{-1}$, after the trigger provided by the probe pulse. Fig. 3c, which displays the calculated evolution (see model below) of τ with the polariton lifetime, confirms that the lifetime of the bullets is almost independent of the injected momentum and it is close to twice the polariton lifetime for our experimental conditions.

An important feature in relation with the prospective use of this system for high rate switching applications is the *on* to *off* switching time at a given point in space. This time is as short as 8 ps, and it is directly determined by the polariton lifetime. Shorter switching times could be obtained in microcavities with lower quality factors, resulting in shorter polariton lifetimes. The price to pay would be an increase of the switching power, as higher powers would be required to generate and maintain the polariton bullet propagation. Additionally, reducing the polariton lifetime would lead to lower signal contrast. Therefore, a compromise between a bigger switching rate and pump power is essential.

Theory. — The spatial dynamics of spinor coherent polaritons can be described by the driven spinor GP equations [20]:

$$i\hbar \frac{\partial \phi_\sigma(\mathbf{x}, t)}{\partial t} = - \left(\frac{\hbar^2 \nabla^2}{2m_C} + \frac{i\hbar}{2\tau_C} \right) \phi_\sigma(\mathbf{x}, t) + V\chi_\sigma(\mathbf{x}, t) + F_\sigma(\mathbf{x}, t) \quad (1)$$

$$i\hbar \frac{\partial \chi_\sigma(\mathbf{x}, t)}{\partial t} = V\phi_\sigma(\mathbf{x}, t) + \left(\Delta - \frac{i\hbar}{2\tau_X} + \alpha_1 |\chi_\sigma(\mathbf{x}, t)|^2 + \alpha_2 |\chi_{-\sigma}(\mathbf{x}, t)|^2 \right) \chi_\sigma(\mathbf{x}, t) \quad (2)$$

where $\phi_\sigma(\mathbf{x}, t)$ and $\chi_\sigma(\mathbf{x}, t)$ represent the cavity photon

and exciton wavefunctions, respectively, which vary in the 2D plane of the microcavity depending on the coordinate \mathbf{x} . $\sigma = \pm 1$ is an index representing the two possible circular polarizations of cavity photons, which couple directly to excitons with spins represented by $\sigma = \pm 1$, respectively. V represents the strength of this coupling. The kinetic energy of cavity photons associated with their in-plane motion is described by a parabolic dispersion with effective mass m_C . We neglect the much higher effective mass of excitons and denote the exciton-photon detuning at zero in-plane wavevector by Δ . Cavity photons are directly pumped by a coherent laser described by the temporally and spatially dependent field $F_\sigma(\mathbf{x}, t)$, which is typically composed of a superposition of *cw* and pulsed pumps. Nonlinear interactions take place between excitons, described by two constants, α_1 and α_2 , which represent the strength of interactions between excitons with parallel and antiparallel spins, respectively.

Starting from the initial condition that the wavefunctions are equal to zero at all points in space, the dynamics of the system can be calculated numerically from Eqs. 1 and 2. This model has been proven to give a good description of polarization sensitive nonlinear experiments in semiconductor microcavities [1, 5, 19]. Solving the GP equations for excitation conditions corresponding to our experiment, we obtain the signal propagation depicted in Figs. 1c and 1d, which reasonably reproduce the experimental behaviour. Using a similar procedure as that for the experimental images, we can extract the dependence of the signal propagation speed on the excitation wavevector, which is shown in Fig. 2. A clear correspondence can be found between the signal propagation speed and the group velocity.

At low wavevectors it is hard to extract a signal propagation speed since the distance travelled by the polariton pulse is minimal. We note that the pump intensity and pump-lower polariton detuning was kept fixed in the calculation of the curve shown in Fig. 2. The fixed pump intensity was chosen below the nonlinear threshold intensity, in agreement with the experimental excitation conditions. As the wavevector decreases the nonlinear

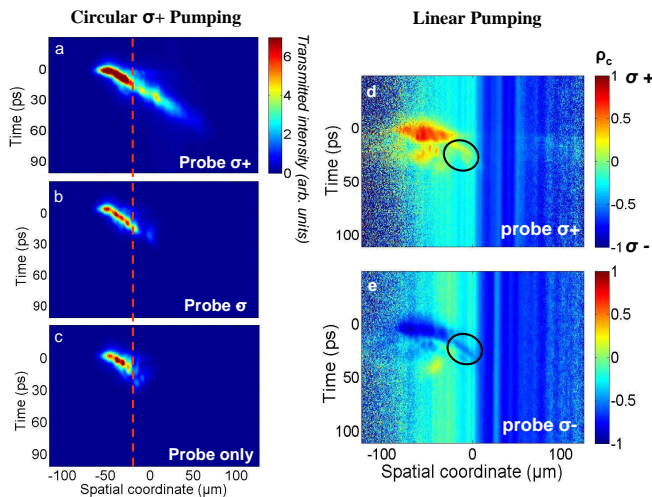


FIG. 4: (a,b,c) Experimental propagation of a bullet when the pump is σ^+ -polarized, with a σ^+ (a) or σ^- (b)-polarized probe, and without the pump (c). The red line is a guide for the eye, evidencing the presence of the switch in the co-polarized case only. (d) and (e) show the degree of circular polarization ρ_c obtained when the pump is almost linearly polarized ($\rho_c^{pump} = -0.2$), with a σ^+ (d) and σ^- (e)-polarized probe. The black circles highlight the part of the signal arising from the switch, which is clearly σ^+ in (d) and σ^- in (e).

threshold increases due to changes in the photonic and excitonic fractions, which decrease the effective polariton lifetime and polariton-polariton interaction strength respectively. Close to $K=0$ (yellow region in Fig. 2) where the non-local effects are less important, our calculations show a bistable behaviour [19] which is not accessible in our experiments as they are performed and stored by averaging over $\sim 10^7$ single pulse realisations (the first pulse causes permanent switching). In this case we should still observe the motion of the switched *on* signal [14], but the propagation speed is expected not to be given by the polariton group velocity but by the gain in energy from the renormalisation converted into kinetic energy. In this way, significant signal speeds could be obtained even if the pump is oriented at normal incidence.

Spin-dependent switching.— Spin bullets of controlled polarization can be prepared taking advantage of the spin dependence of the polariton interactions. In this section we show that we can follow the motion of a polariton bullet of a well-defined spin by adjusting the polarization of the pump and probe beams.

Figures 4a and 4b show raw streak camera images demonstrating the spin sensitivity in the switching of the bullets. Comparing panel (a), where pump and probe polarizations are both σ^+ , with image (b), where they are cross-polarized, we notice that in (a) the bullet propagates a much larger distance and during a much longer time than in case (b). This demonstrates that the switch only happens when the polarizations are the same. This

is further confirmed by comparison with panel (c) which shows that the behaviour of the probe only is identical to that observed in image (b) where polaritons behave as if the pump was absent and spin up polaritons are not significantly affected by spin down polaritons ($|\alpha_1| \gg |\alpha_2|$).

In Figures 4d and 4e we have prepared our *cw* pump in a roughly linear polarization (ellipticity given by $\rho_c^{pump} = -0.2$), and the pulsed probe in σ^+ and σ^- polarizations respectively. The false colour scheme represents the degree of circular polarization ($\rho_c = (I^+ - I^-)/(I^+ + I^-)$, where $I^{+/-}$ is the $\sigma^{+/-}$ right/left circularly polarized emitted intensity), from -1 (blue, σ^-) to +1 (red, σ^+), while green means $\rho_c = 0$, i.e. linear polarization. By adding a σ^+ probe (d), we can observe that a σ^+ polarized spin bullet propagates. A similar behaviour is observed by adding a σ^- probe to the linear pump (e), where now the spin bullet is σ^- .

The reported behaviour under circularly polarised pump and probe conditions of Fig. 4a-c) can be understood in terms of a polarization sensitive intensity switch, whose action propagates all along the pumped area. This shows the great interest of this system for the implementation of multiple gates integrated together in a single semiconductor microcavity in order to make a device for computation, analogous to those suggested in Refs.[21–23].

Conclusion.— This work demonstrates the ultrafast motion of spin bullets in semiconductor microcavities, opening the way for building solid-state spin-optronic logic circuits, operating with high speed and complete integrability. This is a significant step towards realizing optical spin switches [1] and guided transmission of information [14].

We thank R. Houdré for the microcavity sample. This work was supported by the IFRAF, the *Agence Nationale pour la Recherche*, the Spanish *MEC (MAT2008-01555, QOIT-CSD2006-00019)*, *CAM (S-2009/ESP-1503)* and *FP7 ITNs ‘Clermont4’ (235114)*, and *Spin-optonics (237252)*. A.B. is a member of the *Institut Universitaire de France*.

-
- [1] Amo, A. et al., *Nature Photonics* **4**, 361 (2010)
 - [2] Kavokin, A.V., Baumberg, J.J., Malpuech, G., Laussy, F. P., *Microcavities*, Oxford University Press (2007)
 - [3] Martin, M. D. et al., *Phys. Rev. Lett.* **89**, 077402 (2002)
 - [4] Lagoudakis, P. G. et al., *Phys. Rev. B* **65**, 161310 (2002)
 - [5] Leyder, C. et al., *Phys. Rev. Lett.* **99**, 196402 (2007)
 - [6] Gippius, N. A. et al., *Phys. Rev. Lett.* **98**, 236401 (2007)
 - [7] Paraiso, T. K. et al., *Nature Materials* **9**, 655 (2010)
 - [8] Freixanet, T. et al., *Phys. Rev. B* **61**, 7233 (2000)
 - [9] Shelykh, I. A. et al., *Phys. Rev. Lett.* **100**, 116401 (2008)
 - [10] Amo, A. et al., *Nature* **457**, 291 (2009)
 - [11] Johne, R. et al., *Phys. Rev. B* **81**, 125327 (2010)
 - [12] Shelykh, I. A. et al. *Phys. Rev. Lett.* **102**, 046407 (2009)

- [13] Shelykh, I. A. et al., Phys. Rev. B **82**, 153303 (2010)
- [14] Liew, T. C. H. et al., Phys. Rev. Lett. **101**, 016402 (2008)
- [15] Viña, L. et al. Phys. Rev. B **54**, 8317 (1996)
- [16] Vladimirova, M. et al., Phys. Rev. B **82**, 075301 (2010)
- [17] Ciuti, C. et al., Phys. Rev. B **58**, 7926 (1998)
- [18] Kavokin, K.V. et al., Phys. Stat. Sol. (c) **2**, 763 (2005)
- [19] Adrados, C. et al., Phys. Rev. Lett. **105**, 216403 (2010)
- [20] Shelykh, I. A. et al., Phys. Rev. Lett. **97**, 66402 (2006)
- [21] Bouwmeester, D., Ekert, A. K., Zeilinger, A., *The physics of quantum information*, ed. Springer-Verlag Berlin and Heidelberg GmbH & Co. K (2000)
- [22] Wada, O., New J. Phys. **6**, 183 (2004)
- [23] O'Brien, J. L. et al., Nature Photon. **3**, 687 (2009)